University of Groningen

Absolute measurements of branching fractions of Cabibbo-suppressed hadronic D0 (+) decays involving multiple pions

BESIII Collaboration; Kalantar-Nayestanaki, N.; Kappert, R.; Kavatsyuk, M.; Messchendorp, J.; Rodin, V.

Published in:
Physical Review D

DOI:
10.1103/PhysRevD.106.092005

IMPORTANT NOTE: You are advised to consult the publisher's version (publisher's PDF) if you wish to cite from it. Please check the document version below.

Document Version
Publisher's PDF, also known as Version of record

Publication date:
2022

Link to publication in University of Groningen/UMCG research database

Citation for published version (APA):
BESIII Collaboration, Kalantar-Nayestanaki, N., Kappert, R., Kavatsyuk, M., Messchendorp, J., & Rodin, V. (2022). Absolute measurements of branching fractions of Cabibbo-suppressed hadronic D0 (+) decays involving multiple pions. *Physical Review D*, *106*(9), Article 092005. https://doi.org/10.1103/PhysRevD.106.092005

Copyright
Other than for strictly personal use, it is not permitted to download or to forward/distribute the text or part of it without the consent of the author(s) and/or copyright holder(s), unless the work is under an open content license (like Creative Commons).

The publication may also be distributed here under the terms of Article 25fa of the Dutch Copyright Act, indicated by the “Taverne” license. More information can be found on the University of Groningen website: https://www.rug.nl/library/open-access/self-archiving-pure/taverne-amendment.

Take-down policy
If you believe that this document breaches copyright please contact us providing details, and we will remove access to the work immediately and investigate your claim.

Downloaded from the University of Groningen/UMCG research database (Pure): http://www.rug.nl/research/portal. For technical reasons the number of authors shown on this cover page is limited to 10 maximum.

PHYSICAL REVIEW D **106,** 092005 (2022)

Absolute measurements of branching fractions of Cabibbo-suppressed hadronic $D^{0(+)}$ decays involving multiple pions

M. Ablikim,[1] M. N. Achasov,[11,b] P. Adlarson,[71] M. Albrecht,[4] R. Aliberti,[31] A. Amoroso,[70a,70c] M. R. An,[35] Q. An,[67,53]
X. H. Bai,[61] Y. Bai,[52] O. Bakina,[32] R. Baldini Ferroli,[26a] I. Balossino,[27a] Y. Ban,[42,g] V. Batozskaya,[1,40] D. Becker,[31]
K. Begzsuren,[29] N. Berger,[31] M. Bertani,[26a] D. Bettoni,[27a] F. Bianchi,[70a,70c] J. Bloms,[64] A. Bortone,[70a,70c] I. Boyko,[32]
R. A. Briere,[5] A. Brueggemann,[64] H. Cai,[72] X. Cai,[1,53] A. Calcaterra,[26a] G. F. Cao,[1,58] N. Cao,[1,58] S. A. Cetin,[57a]
J. F. Chang,[1,53] W. L. Chang,[1,58] G. Chelkov,[32,a] C. Chen,[39] G. Chen,[1] H. S. Chen,[1,58] M. L. Chen,[1,53] S. J. Chen,[38] T. Chen,[1]
X. R. Chen,[28,58] X. T. Chen,[1] Y. B. Chen,[1,53] Z. J. Chen,[23,h] W. S. Cheng,[70c] X. Chu,[39] G. Cibinetto,[27a] F. Cossio,[70c]
J. J. Cui,[45] H. L. Dai,[1,53] J. P. Dai,[74] A. Dbeyssi,[17] R. E. de Boer,[4] D. Dedovich,[32] Z. Y. Deng,[1] A. Denig,[31] I. Denysenko,[32]
M. Destefanis,[70a,70c] F. De Mori,[70a,70c] Y. Ding,[36] J. Dong,[1,53] L. Y. Dong,[1,58] M. Y. Dong,[1,53,58] X. Dong,[72] S. X. Du,[76]
P. Egorov,[32,a] Y. L. Fan,[72] J. Fang,[1,53] S. S. Fang,[1,58] W. X. Fang,[1] Y. Fang,[1] R. Farinelli,[27a] L. Fava,[70b,70c] F. Feldbauer,[4]
G. Felici,[26a] C. Q. Feng,[67,53] J. H. Feng,[54] K. Fischer,[65] M. Fritsch,[4] C. Fritzsch,[64] C. D. Fu,[1] H. Gao,[58] Y. N. Gao,[42,g]
Yang Gao,[67,53] S. Garbolino,[70c] I. Garzia,[27a,27b] P. T. Ge,[72] Z. W. Ge,[38] C. Geng,[54] E. M. Gersabeck,[62] A. Gilman,[65]
K. Goetzen,[12] L. Gong,[36] W. X. Gong,[1,53] W. Gradl,[31] M. Greco,[70a,70c] L. M. Gu,[38] M. H. Gu,[1,53] Y. T. Gu,[14] C. Y. Guan,[1,58]
A. Q. Guo,[28,58] L. B. Guo,[37] R. P. Guo,[44] Y. P. Guo,[10,f] A. Guskov,[32,a] T. T. Han,[45] W. Y. Han,[35] X. Q. Hao,[18] F. A. Harris,[60]
K. K. He,[50] K. L. He,[1,58] F. H. Heinsius,[4] C. H. Heinz,[31] Y. K. Heng,[1,53,58] C. Herold,[55] M. Himmelreich,[12,d] T. Holtmann,[4]
G. Y. Hou,[1,58] Y. R. Hou,[58] Z. L. Hou,[1] H. M. Hu,[1,58] J. F. Hu,[51,i] T. Hu,[1,53,58] Y. Hu,[1] G. S. Huang,[67,53] K. X. Huang,[54]
L. Q. Huang,[28,58] L. Q. Huang,[68] X. T. Huang,[45] Y. P. Huang,[1] Z. Huang,[42,g] T. Hussain,[69] N. Hüsken,[25,31] W. Imoehl,[25]
M. Irshad,[67,53] J. Jackson,[25] S. Jaeger,[4] S. Janchiv,[29] Q. Ji,[1] Q. P. Ji,[18] X. B. Ji,[1,58] X. L. Ji,[1,53] Y. Y. Ji,[45] Z. K. Jia,[67,53]
H. B. Jiang,[45] S. S. Jiang,[35] X. S. Jiang,[1,53,58] Y. Jiang,[58] J. B. Jiao,[45] Z. Jiao,[21] S. Jin,[38] Y. Jin,[61] M. Q. Jing,[1,58]
T. Johansson,[71] N. Kalantar-Nayestanaki,[59] X. S. Kang,[36] R. Kappert,[59] M. Kavatsyuk,[59] B. C. Ke,[76] I. K. Keshk,[4]
A. Khoukaz,[64] P. Kiese,[31] R. Kiuchi,[1] R. Kliemt,[12] L. Koch,[33] O. B. Kolcu,[57a] B. Kopf,[4] M. Kuemmel,[4] M. Kuessner,[4]
A. Kupsc,[40,71] W. Kühn,[33] J. J. Lane,[62] J. S. Lange,[33] P. Larin,[17] A. Lavania,[24] L. Lavezzi,[70a,70c] Z. H. Lei,[67,53] H. Leithoff,[31]
M. Lellmann,[31] T. Lenz,[31] C. Li,[43] C. Li,[39] C. H. Li,[35] Cheng Li,[67,53] D. M. Li,[76] F. Li,[1,53] G. Li,[1] H. Li,[47] H. Li,[67,53]
H. B. Li,[1,58] H. J. Li,[18] H. N. Li,[51,i] J. Q. Li,[4] J. S. Li,[54] J. W. Li,[45] Ke Li,[1] L. J. Li,[1] L. K. Li,[1] Lei Li,[3] M. H. Li,[39] P. R. Li,[34,j,k]
S. X. Li,[10] S. Y. Li,[56] T. Li,[45] W. D. Li,[1,58] W. G. Li,[1] X. H. Li,[67,53] X. L. Li,[45] Xiaoyu Li,[1,58] H. Liang,[67,53] H. Liang,[30]
H. Liang,[1,58] Y. F. Liang,[49] Y. T. Liang,[28,58] G. R. Liao,[13] L. Z. Liao,[45] J. Libby,[24] A. Limphirat,[55] C. X. Lin,[54] D. X. Lin,[28,58]
T. Lin,[1] B. J. Liu,[1] C. X. Liu,[1] D. Liu,[17,67] F. H. Liu,[48] Fang Liu,[1] Feng Liu,[6] G. M. Liu,[51,i] H. Liu,[34,j,k] H. B. Liu,[14]
H. M. Liu,[1,58] Huanhuan Liu,[1] Huihui Liu,[19] J. B. Liu,[67,53] J. L. Liu,[68] J. Y. Liu,[1,58] K. Liu,[1] K. Y. Liu,[36] Ke Liu,[20] L. Liu,[67,53]
Lu Liu,[39] M. H. Liu,[10,f] P. L. Liu,[1] Q. Liu,[58] S. B. Liu,[67,53] T. Liu,[10,f] W. K. Liu,[39] W. M. Liu,[67,53] X. Liu,[34,j,k] Y. Liu,[34,j,k]
Y. B. Liu,[39] Z. A. Liu,[1,53,58] Z. Q. Liu,[45] X. C. Lou,[1,53,58] F. X. Lu,[54] H. J. Lu,[21] J. G. Lu,[1,53] X. L. Lu,[1] Y. Lu,[7] Y. P. Lu,[1,53]
Z. H. Lu,[1] C. L. Luo,[37] M. X. Luo,[75] T. Luo,[10,f] X. L. Luo,[1,53] X. R. Lyu,[58] Y. F. Lyu,[39] F. C. Ma,[36] H. L. Ma,[1] L. L. Ma,[45]
M. M. Ma,[1,58] Q. M. Ma,[1] R. Q. Ma,[1,58] R. T. Ma,[58] X. Y. Ma,[1,53] Y. Ma,[42,g] F. E. Maas,[17] M. Maggiora,[70a,70c] S. Maldaner,[4]
S. Malde,[65] Q. A. Malik,[69] A. Mangoni,[26b] Y. J. Mao,[42,g] Z. P. Mao,[1] S. Marcello,[70a,70c] Z. X. Meng,[61]
J. G. Messchendorp,[59,12] G. Mezzadri,[27a] H. Miao,[1] T. J. Min,[38] R. E. Mitchell,[25] X. H. Mo,[1,53,58] N. Yu. Muchnoi,[11,b]
H. Muramatsu,[63] Y. Nefedov,[32] F. Nerling,[12,d] I. B. Nikolaev,[11,b] Z. Ning,[1,53] S. Nisar,[9,l] Y. Niu,[45] S. L. Olsen,[58]
Q. Ouyang,[1,53,58] S. Pacetti,[26b,26c] X. Pan,[10,f] Y. Pan,[62] A. Pathak,[30] M. Pelizaeus,[4] H. P. Peng,[67,53] K. Peters,[12,d] J. L. Ping,[37]
R. G. Ping,[1,58] S. Plura,[31] S. Pogodin,[32] R. Poling,[63] V. Prasad,[67,53] F. Z. Qi,[1] H. Qi,[67,53] H. R. Qi,[56] M. Qi,[38] T. Y. Qi,[10,f]
S. Qian,[1,53] W. B. Qian,[58] Z. Qian,[54] C. F. Qiao,[58] J. J. Qin,[68] L. Q. Qin,[13] X. P. Qin,[10,f] X. S. Qin,[45] Z. H. Qin,[1,53] J. F. Qiu,[1]
S. Q. Qu,[56] K. H. Rashid,[69] C. F. Redmer,[31] K. J. Ren,[35] A. Rivetti,[70c] V. Rodin,[59] M. Rolo,[70c] G. Rong,[1,58] Ch. Rosner,[17]
S. N. Ruan,[39] H. S. Sang,[67] A. Sarantsev,[32,c] Y. Schelhaas,[31] C. Schnier,[4] K. Schoenning,[71] M. Scodeggio,[27a,27b]
K. Y. Shan,[10,f] W. Shan,[22] X. Y. Shan,[67,53] J. F. Shangguan,[50] L. G. Shao,[1,58] M. Shao,[67,53] C. P. Shen,[10,f] H. F. Shen,[1,58]
X. Y. Shen,[1,58] B. A. Shi,[58] H. C. Shi,[67,53] J. Y. Shi,[1] R. S. Shi,[1,58] X. Shi,[1,53] X. D. Shi,[67,53] J. J. Song,[18] W. M. Song,[30,1]
Y. X. Song,[42,g] S. Sosio,[70a,70c] S. Spataro,[70a,70c] F. Stieler,[31] K. X. Su,[72] P. P. Su,[50] Y. J. Su,[58] G. X. Sun,[1] H. Sun,[58]
H. K. Sun,[1] J. F. Sun,[18] L. Sun,[72] S. S. Sun,[1,58] T. Sun,[1,58] W. Y. Sun,[30] X. Sun,[23,h] Y. J. Sun,[67,53] Y. Z. Sun,[1] Z. T. Sun,[45]
Y. H. Tan,[72] Y. X. Tan,[67,53] C. J. Tang,[49] G. Y. Tang,[1] J. Tang,[54] L. Y. Tao,[68] Q. T. Tao,[23,h] J. X. Teng,[67,53] V. Thoren,[71]
W. H. Tian,[47] Y. Tian,[28,58] I. Uman,[57b] B. Wang,[1] B. L. Wang,[58] C. W. Wang,[38] D. Y. Wang,[42,g] F. Wang,[68] H. J. Wang,[34,j,k]
H. P. Wang,[1,58] K. Wang,[1,53] L. L. Wang,[1] M. Wang,[45] M. Z. Wang,[42,g] Meng Wang,[1,58] S. Wang,[13] S. Wang,[10,f] T. Wang,[10,f]
T. J. Wang,[39] W. Wang,[54] W. H. Wang,[72] W. P. Wang,[67,53] X. Wang,[42,g] X. F. Wang,[34,j,k] X. L. Wang,[10,f] Y. D. Wang,[41]
Y. F. Wang,[1,53,58] Y. H. Wang,[43] Y. Q. Wang,[1] Yaqian Wang,[16,1] Z. Wang,[1,53] Z. Y. Wang,[1,58] Ziyi Wang,[58] D. H. Wei,[13]

2470-0010/2022/106(9)/092005(11)

Published by the American Physical Society

F. Weidner,[64] S. P. Wen,[1] D. J. White,[62] U. Wiedner,[4] G. Wilkinson,[65] M. Wolke,[71] L. Wollenberg,[4] J. F. Wu,[1,58] L. H. Wu,[1] L. J. Wu,[1,58] X. Wu,[10,f] X. H. Wu,[30] Y. Wu,[67] Y. J. Wu,[28] Z. Wu,[1,53] L. Xia,[67,53] T. Xiang,[42,g] D. Xiao,[34,j,k] G. Y. Xiao,[38] H. Xiao,[10,f] S. Y. Xiao,[1] Y. L. Xiao,[10,f] Z. J. Xiao,[37] C. Xie,[38] X. H. Xie,[42,g] Y. Xie,[45] Y. G. Xie,[1,53] Y. H. Xie,[6] Z. P. Xie,[67,53] T. Y. Xing,[1,58] C. F. Xu,[1] C. J. Xu,[54] G. F. Xu,[1] H. Y. Xu,[61] Q. J. Xu,[15] X. P. Xu,[50] Y. C. Xu,[58] Z. P. Xu,[38] F. Yan,[10,f] L. Yan,[10,f] W. B. Yan,[67,53] W. C. Yan,[76] H. J. Yang,[46,e] H. L. Yang,[30] H. X. Yang,[1] L. Yang,[47] S. L. Yang,[58] Tao Yang,[1] Y. F. Yang,[39] Y. X. Yang,[1,58] Yifan Yang,[1,58] M. Ye,[1,53] M. H. Ye,[8] J. H. Yin,[1] Z. Y. You,[54] B. X. Yu,[1,53,58] C. X. Yu,[39] G. Yu,[1,58] T. Yu,[68] C. Z. Yuan,[1,58] L. Yuan,[2] S. C. Yuan,[1] X. Q. Yuan,[1] Y. Yuan,[1,58] Z. Y. Yuan,[54] C. X. Yue,[35] A. A. Zafar,[69] F. R. Zeng,[45] X. Zeng,[6] Y. Zeng,[23,h] Y. H. Zhan,[54] A. Q. Zhang,[1] B. L. Zhang,[1] B. X. Zhang,[1] D. H. Zhang,[39] G. Y. Zhang,[18] H. Zhang,[67] H. H. Zhang,[30] H. H. Zhang,[54] H. Y. Zhang,[1,53] J. L. Zhang,[73] J. Q. Zhang,[37] J. W. Zhang,[1,53,58] J. X. Zhang,[34,j,k] J. Y. Zhang,[1] J. Z. Zhang,[1,58] Jianyu Zhang,[1,58] Jiawei Zhang,[1,58] L. M. Zhang,[56] L. Q. Zhang,[54] Lei Zhang,[38] P. Zhang,[1] Q. Y. Zhang,[35,76] Shuihan Zhang,[1,58] Shulei Zhang,[23,h] X. D. Zhang,[41] X. M. Zhang,[1] X. Y. Zhang,[45] X. Y. Zhang,[50] Y. Zhang,[65] Y. T. Zhang,[76] Y. H. Zhang,[1,53] Yan Zhang,[67,53] Yao Zhang,[1] Z. H. Zhang,[1] Z. Y. Zhang,[72] Z. Y. Zhang,[39] G. Zhao,[1] J. Zhao,[35] J. Y. Zhao,[1,58] J. Z. Zhao,[1,53] Lei Zhao,[67,53] Ling Zhao,[1] M. G. Zhao,[39] Q. Zhao,[1] S. J. Zhao,[76] Y. B. Zhao,[1,53] Y. X. Zhao,[28,58] Z. G. Zhao,[67,53] A. Zhemchugov,[32,a] B. Zheng,[68] J. P. Zheng,[1,53] Y. H. Zheng,[58] B. Zhong,[37] C. Zhong,[68] X. Zhong,[54] H. Zhou,[45] L. P. Zhou,[1,58] X. Zhou,[72] X. K. Zhou,[58] X. R. Zhou,[67,53] X. Y. Zhou,[35] Y. Z. Zhou,[10,f] J. Zhu,[39] K. Zhu,[1] K. J. Zhu,[1,53,58] L. X. Zhu,[58] S. H. Zhu,[66] S. Q. Zhu,[38] T. J. Zhu,[73] W. J. Zhu,[10,f] Y. C. Zhu,[67,53] Z. A. Zhu,[1,58] B. S. Zou,[1] and J. H. Zou[1]

(BESIII Collaboration)

[1]*Institute of High Energy Physics, Beijing 100049, People's Republic of China*
[2]*Beihang University, Beijing 100191, People's Republic of China*
[3]*Beijing Institute of Petrochemical Technology, Beijing 102617, People's Republic of China*
[4]*Bochum Ruhr-University, D-44780 Bochum, Germany*
[5]*Carnegie Mellon University, Pittsburgh, Pennsylvania 15213, USA*
[6]*Central China Normal University, Wuhan 430079, People's Republic of China*
[7]*Central South University, Changsha 410083, People's Republic of China*
[8]*China Center of Advanced Science and Technology, Beijing 100190, People's Republic of China*
[9]*COMSATS University Islamabad, Lahore Campus, Defence Road,*
Off Raiwind Road, 54000 Lahore, Pakistan
[10]*Fudan University, Shanghai 200433, People's Republic of China*
[11]*G.I. Budker Institute of Nuclear Physics SB RAS (BINP), Novosibirsk 630090, Russia*
[12]*GSI Helmholtzcentre for Heavy Ion Research GmbH, D-64291 Darmstadt, Germany*
[13]*Guangxi Normal University, Guilin 541004, People's Republic of China*
[14]*Guangxi University, Nanning 530004, People's Republic of China*
[15]*Hangzhou Normal University, Hangzhou 310036, People's Republic of China*
[16]*Hebei University, Baoding 071002, People's Republic of China*
[17]*Helmholtz Institute Mainz, Staudinger Weg 18, D-55099 Mainz, Germany*
[18]*Henan Normal University, Xinxiang 453007, People's Republic of China*
[19]*Henan University of Science and Technology, Luoyang 471003, People's Republic of China*
[20]*Henan University of Technology, Zhengzhou 450001, People's Republic of China*
[21]*Huangshan College, Huangshan 245000, People's Republic of China*
[22]*Hunan Normal University, Changsha 410081, People's Republic of China*
[23]*Hunan University, Changsha 410082, People's Republic of China*
[24]*Indian Institute of Technology Madras, Chennai 600036, India*
[25]*Indiana University, Bloomington, Indiana 47405, USA*
[26a]*INFN Laboratori Nazionali di Frascati, I-00044 Frascati, Italy*
[26b]*INFN Sezione di Perugia, I-06100 Perugia, Italy*
[26c]*University of Perugia, I-06100 Perugia, Italy*
[27a]*INFN Sezione di Ferrara, I-44122 Ferrara, Italy*
[27b]*University of Ferrara, I-44122 Ferrara, Italy*
[28]*Institute of Modern Physics, Lanzhou 730000, People's Republic of China*
[29]*Institute of Physics and Technology, Peace Avenue 54B, Ulaanbaatar 13330, Mongolia*
[30]*Jilin University, Changchun 130012, People's Republic of China*
[31]*Johannes Gutenberg University of Mainz, Johann-Joachim-Becher-Weg 45, D-55099 Mainz, Germany*
[32]*Joint Institute for Nuclear Research, 141980 Dubna, Moscow region, Russia*

[33]*Justus-Liebig-Universitaet Giessen, II. Physikalisches Institut, Heinrich-Buff-Ring 16,*
D-35392 Giessen, Germany
[34]*Lanzhou University, Lanzhou 730000, People's Republic of China*
[35]*Liaoning Normal University, Dalian 116029, People's Republic of China*
[36]*Liaoning University, Shenyang 110036, People's Republic of China*
[37]*Nanjing Normal University, Nanjing 210023, People's Republic of China*
[38]*Nanjing University, Nanjing 210093, People's Republic of China*
[39]*Nankai University, Tianjin 300071, People's Republic of China*
[40]*National Centre for Nuclear Research, Warsaw 02-093, Poland*
[41]*North China Electric Power University, Beijing 102206, People's Republic of China*
[42]*Peking University, Beijing 100871, People's Republic of China*
[43]*Qufu Normal University, Qufu 273165, People's Republic of China*
[44]*Shandong Normal University, Jinan 250014, People's Republic of China*
[45]*Shandong University, Jinan 250100, People's Republic of China*
[46]*Shanghai Jiao Tong University, Shanghai 200240, People's Republic of China*
[47]*Shanxi Normal University, Linfen 041004, People's Republic of China*
[48]*Shanxi University, Taiyuan 030006, People's Republic of China*
[49]*Sichuan University, Chengdu 610064, People's Republic of China*
[50]*Soochow University, Suzhou 215006, People's Republic of China*
[51]*South China Normal University, Guangzhou 510006, People's Republic of China*
[52]*Southeast University, Nanjing 211100, People's Republic of China*
[53]*State Key Laboratory of Particle Detection and Electronics,*
Beijing 100049, Hefei 230026, People's Republic of China
[54]*Sun Yat-Sen University, Guangzhou 510275, People's Republic of China*
[55]*Suranaree University of Technology, University Avenue 111, Nakhon Ratchasima 30000, Thailand*
[56]*Tsinghua University, Beijing 100084, People's Republic of China*
[57a]*Turkish Accelerator Center Particle Factory Group, Istinye University, 34010 Istanbul, Turkey*
[57b]*Near East University, Nicosia, North Cyprus, Mersin 10, Turkey*
[58]*University of Chinese Academy of Sciences, Beijing 100049, People's Republic of China*
[59]*University of Groningen, NL-9747 AA Groningen, The Netherlands*
[60]*University of Hawaii, Honolulu, Hawaii 96822, USA*
[61]*University of Jinan, Jinan 250022, People's Republic of China*
[62]*University of Manchester, Oxford Road, Manchester M13 9PL, United Kingdom*
[63]*University of Minnesota, Minneapolis, Minnesota 55455, USA*
[64]*University of Muenster, Wilhelm-Klemm-Strasse 9, 48149 Muenster, Germany*
[65]*University of Oxford, Keble Road, Oxford OX13RH, United Kingdom*
[66]*University of Science and Technology Liaoning, Anshan 114051, People's Republic of China*
[67]*University of Science and Technology of China, Hefei 230026, People's Republic of China*
[68]*University of South China, Hengyang 421001, People's Republic of China*
[69]*University of the Punjab, Lahore-54590, Pakistan*
[70a]*University of Turin and INFN, University of Turin, I-10125 Turin, Italy*
[70b]*University of Eastern Piedmont, I-15121 Alessandria, Italy*
[70c]*INFN, I-10125 Turin, Italy*
[71]*Uppsala University, Box 516, SE-75120 Uppsala, Sweden*
[72]*Wuhan University, Wuhan 430072, People's Republic of China*
[73]*Xinyang Normal University, Xinyang 464000, People's Republic of China*
[74]*Yunnan University, Kunming 650500, People's Republic of China*
[75]*Zhejiang University, Hangzhou 310027, People's Republic of China*
[76]*Zhengzhou University, Zhengzhou 450001, People's Republic of China*

---

[a] Also at the Moscow Institute of Physics and Technology, Moscow 141700, Russia.

[b] Also at the Novosibirsk State University, Novosibirsk 630090, Russia.

[c] Also at the NRC "Kurchatov Institute," PNPI, 188300 Gatchina, Russia.

[d] Also at Goethe University Frankfurt, 60323 Frankfurt am Main, Germany.

[e] Also at Key Laboratory for Particle Physics, Astrophysics and Cosmology, Ministry of Education; Shanghai Key Laboratory for Particle Physics and Cosmology; Institute of Nuclear and Particle Physics, Shanghai 200240, People's Republic of China.

[f] Also at Key Laboratory of Nuclear Physics and Ion-beam Application (MOE) and Institute of Modern Physics, Fudan University, Shanghai 200443, People's Republic of China.

[g] Also at State Key Laboratory of Nuclear Physics and Technology, Peking University, Beijing 100871, People's Republic of China.

[h] Also at School of Physics and Electronics, Hunan University, Changsha 410082, China.

(Received 29 June 2022; accepted 27 October 2022; published 23 November 2022)

By analyzing e^+e^- annihilation data with an integrated luminosity of 2.93 fb^{-1} collected at the center-of-mass energy $\sqrt{s} = 3.773$ GeV with the BESIII detector, we present the first absolute measurements of the branching fractions of twenty Cabibbo-suppressed hadronic $D^{0(+)}$ decays involving multiple pions. The highest four branching fractions obtained are $\mathcal{B}(D^0 \to \pi^+\pi^-\pi^0) = (1.343 \pm 0.013_{\mathrm{stat}} \pm 0.016_{\mathrm{syst}})\%$, $\mathcal{B}(D^0 \to \pi^+\pi^-2\pi^0) = (1.002 \pm 0.019_{\mathrm{stat}} \pm 0.024_{\mathrm{syst}})\%$, $\mathcal{B}(D^+ \to 2\pi^+\pi^-\pi^0) = (1.165 \pm 0.021_{\mathrm{stat}} \pm 0.021_{\mathrm{syst}})\%$, and $\mathcal{B}(D^+ \to 2\pi^+\pi^-2\pi^0) = (1.074 \pm 0.040_{\mathrm{stat}} \pm 0.030_{\mathrm{syst}})\%$. The CP asymmetries for the six decays with highest signal yields are also determined and found to be compatible with zero.

DOI: 10.1103/PhysRevD.106.092005

I. INTRODUCTION

Investigations of hadronic $D^{0(+)}$ decays are of general importance for both charm and bottom physics. For example, Ref. [1] suggests that hadronic $D^{0(+)}$ decays involving three charged pions are crucial backgrounds for the tests of lepton flavor universality (LFU) in semileptonic B decays. However, many Cabibbo-suppressed hadronic $D^{0(+)}$ decays with three charged pions are unexplored mainly due to low detection efficiencies and high background contamination. Precision and comprehensive measurements of the absolute branching fractions (BFs) of these decays provide necessary inputs to unravel the hints of LFU violation observed in semileptonic B decays.

According to theoretical predictions, direct CP violation in charmed hadron decays is expected to be at the order of 10^{-3} for singly Cabibbo-suppressed processes, and much smaller for Cabibbo-favored and doubly Cabibbo-suppressed processes [2–9]. The LHCb experiment reported the first observation of CP violation in $D^0 \to K^+K^-$ and $\pi^+\pi^-$ with an asymmetry difference of $\Delta A_{CP} = (1.54 \pm 0.29) \times 10^{-3}$ [10]. A similar magnitude of CP asymmetry is predicted in $D^0 \to K^+K^{*-}$ and $D^0 \to \rho^+\pi^-$ [8]. References [2,3] suggest that the CP asymmetries in $D \to \rho\pi$ decays are in the range of $(0.3 \sim 5) \times 10^{-4}$. Therefore, searching for CP violation in Cabibbo-suppressed $D^{0(+)}$ decays into three pions is an interesting pursuit.

The Cabibbo-suppressed hadronic neutral D decays into $\pi^+\pi^-\pi^0$ and $\pi^+\pi^-\pi^0\pi^0$ also provide a promising way to extract the Cabibbo-Kobayashi-Maskawa angle γ in $B^+ \to D^{(*)0}K^{(*)+}$ [11]. More precise measurements of these BFs or improved knowledge of CP-even fractions can improve the measurement precision for the CP violation phase angle γ with these modes.

This paper reports the first absolute measurements of the BFs of the Cabibbo-suppressed hadronic decays $D^0 \to \pi^+\pi^-\pi^0$, $\pi^+\pi^-2\pi^0$, $\pi^+\pi^-2\eta$, $4\pi^0$, $3\pi^0\eta$, $2\pi^+2\pi^-\pi^0$, $2\pi^+2\pi^-\eta$, $\pi^+\pi^-3\pi^0$, $2\pi^+2\pi^-2\pi^0$, and $D^+ \to 2\pi^+\pi^-$, $\pi^+2\pi^0$, $2\pi^+\pi^-\pi^0$, $\pi^+3\pi^0$, $3\pi^+2\pi^-$, $2\pi^+\pi^-2\pi^0$, $2\pi^+\pi^-\pi^0\eta$, $\pi^+4\pi^0$, $\pi^+3\pi^0\eta$, $3\pi^+2\pi^-\pi^0$, $2\pi^+\pi^-3\pi^0$ based on 2.93 fb^{-1} of e^+e^- annihilation data taken at the center-of-mass energy $\sqrt{s} = 3.773$ GeV with the BESIII detector [12]. Moreover, the CP asymmetries for the six decays with the highest yields are determined. To date, only the BFs of seven of these decay modes have been measured relative to reference modes and only the CP asymmetries in $D^0(\bar{D}^0) \to \pi^+\pi^-\pi^0$ and $D^\pm \to \pi^+\pi^-\pi^\pm$ have been measured by various experiments [13]. Throughout this article, charge-conjugated processes are implied except when discussing CP asymmetries.

II. BESIII AND MONTE CARLO SIMULATION

The BESIII detector is a magnetic spectrometer [14] located at the Beijing Electron Positron Collider (BEPCII) [15]. The cylindrical core of the BESIII detector consists of a helium-based multilayer drift chamber, a plastic scintillator time-of-flight system (TOF), and a CsI (Tl) electromagnetic calorimeter (EMC), which are all enclosed in a superconducting solenoidal magnet providing a 1.0 T magnetic field. The solenoid is supported by an octagonal flux-return yoke with resistive-plate counter muon-identifier modules interleaved with steel. The acceptance of charged particles and photons is 93% over 4π solid angle. The charged-particle momentum resolution at 1 GeV$/c$ is 0.5%, and the resolution of the specific ionization energy loss (dE/dx) is 6% for the electrons from Bhabha scattering. The EMC measures photon energies with a resolution of 2.5% (5%) at 1 GeV in the

---

[i] Also at Guangdong Provincial Key Laboratory of Nuclear Science, Institute of Quantum Matter, South China Normal University, Guangzhou 510006, China.

[j] Also at Frontiers Science Center for Rare Isotopes, Lanzhou University, Lanzhou 730000, People's Republic of China.

[k] Also at Lanzhou Center for Theoretical Physics, Lanzhou University, Lanzhou 730000, People's Republic of China.

[l] Also at the Department of Mathematical Sciences, IBA, Karachi 75270, Pakistan.

Published by the American Physical Society under the terms of the Creative Commons Attribution 4.0 International license. Further distribution of this work must maintain attribution to the author(s) and the published article's title, journal citation, and DOI. Funded by SCOAP^3.

barrel (end cap) region. The time resolution of the TOF barrel part is 68 ps, while that of the end cap part is 110 ps.

Simulated samples produced with a GEANT4-based [16] Monte Carlo (MC) package including the geometric description of the BESIII detector and the detector response, are used to determine the detection efficiencies and to estimate backgrounds. The simulation of e^+e^- annihilations modeled with the generator KKMC [17] includes the beam-energy spread and initial-state radiation. The inclusive MC samples consist of the production of $D\bar{D}$ pairs with consideration of quantum coherence for all neutral D modes, the non-$D\bar{D}$ decays of the $\psi(3770)$, the initial-state radiation production of the J/ψ and $\psi(3686)$ states, and continuum processes. Known decay modes are modeled with EVTGEN [18] using the BFs taken from Ref. [13], and the remaining unknown decays of the charmonium states are modeled with LUNDCHARM [19,20]. Final-state radiation from charged final-state particles is incorporated using PHOTOS [21].

III. MEASUREMENT METHOD

At $\sqrt{s} = 3.773$ GeV, the $D^0\bar{D}^0$ or D^+D^- pairs are produced without accompanying hadron(s), thereby offering a clean environment to investigate hadronic D decays with the double-tag (DT) method [22]. The single-tag (ST) $\bar{D}$ candidates are selected by reconstructing a $\bar{D}^0$ or D^- in the hadronic decay modes: $\bar{D}^0 \to K^+\pi^-$, $K^+\pi^-\pi^0$, and $K^+\pi^-\pi^-\pi^+$, and $D^- \to K^+\pi^-\pi^-$, $K^0_S\pi^-$, $K^+\pi^-\pi^-\pi^0$, $K^0_S\pi^-\pi^0$, $K^0_S\pi^+\pi^-\pi^-$, and $K^+K^-\pi^-$. Events in which a signal candidate is reconstructed in the presence of an ST $\bar{D}$ meson are referred to as DT events. The BF of the signal decay is determined by [23]

$$\mathcal{B}_{\rm sig} = N_{\rm DT}/(N^{\rm tot}_{\rm ST} \cdot \epsilon_{\rm sig}), \tag{1}$$

where $N^{\rm tot}_{\rm ST} = \sum_i N^i_{\rm ST}$ and $N_{\rm DT}$ are the total yields of the ST and DT candidates in data, respectively. The ST yield for the tag mode i is $N^i_{\rm ST}$, and the efficiency $\epsilon_{\rm sig}$ for detecting the signal D decay is averaged over the tag modes i.

IV. DATA ANALYSIS

The selection criteria of $K^\pm$, $\pi^\pm$, K^0_S, π^0, and η are the same as those used in the analyses presented in Refs. [23,24]. For $\bar{D}^0 \to K^+\pi^-$, the backgrounds from cosmic rays and Bhabha events are rejected by using the same requirements described in Ref. [25]. For $\bar{D}^0 \to K^+\pi^-\pi^-\pi^+$, the $\bar{D}^0 \to K^0_S K^\pm\pi^\mp$ decays are suppressed by requiring the invariant masses of all $\pi^+\pi^-$ pairs to be outside the mass window $(0.483, 0.513)$ GeV$/c^2$.

Tagged $\bar{D}$ mesons are identified using two variables: the energy difference $\Delta E_{\rm tag} \equiv E_{\rm tag} - E_{\rm b}$ and the beam-constrained mass $M^{\rm tag}_{\rm BC} \equiv \sqrt{E^2_{\rm b} - |\vec{p}_{\rm tag}|^2}$. Here, $E_{\rm b}$ is the beam energy, $\vec{p}_{\rm tag}$ and $E_{\rm tag}$ are the momentum and energy of $\bar{D}$ in the rest frame of e^+e^- system, respectively. The $\Delta E_{\rm tag}$ of ST $\bar{D}$ candidates must be in the range $(-55, 40)$ MeV for the tag modes involving π^0 and $(-25, 25)$ MeV for the other tag modes, due to differing resolutions. For each tag mode, if there are multiple candidates in an event, only the one yielding the least $|\Delta E_{\rm tag}|$ is accepted.

To extract the yields of ST $\bar{D}$ candidates for individual tag modes, binned maximum-likelihood fits are performed to the corresponding $M^{\rm tag}_{\rm BC}$ distributions of the accepted ST candidates following Ref. [24]. The $\bar{D}$ signal is modeled by an MC-simulated shape convolved with a double-Gaussian function describing the resolution difference between the data and MC simulation. The combinatorial background shape is described by an ARGUS function [26]. The total yields of the ST $\bar{D}^0$ and D^- candidates in data are $(232.8 \pm 0.2_{\rm stat}) \times 10^4$ and $(155.8 \pm 0.2_{\rm stat}) \times 10^4$, respectively.

The signal D decays are selected from the remaining tracks and showers recoiling against the tagged $\bar{D}$ candidates. To reject the main backgrounds from Cabibbo-suppressed decays containing K^0_S, the $\pi^+\pi^-$ and $\pi^0\pi^0$ combinations are required to not fall in the mass windows $(0.468,\ 0.528)$ and $(0.428, 0.548)$ GeV$/c^2$, respectively. These mass windows correspond to at least 4σ of resolution.

Signal D mesons are identified using the energy difference $\Delta E_{\rm sig}$ and the beam-constrained mass $M^{\rm sig}_{\rm BC}$, calculated similarly to the ST side. For each signal mode, if there are multiple candidates in an event, only the one with the minimum $|\Delta E_{\rm sig}|$ is chosen. Signal decays are required to satisfy the $\Delta E_{\rm sig}$ requirements shown in Table I.

For each signal decay mode, the signal yield ($N_{\rm DT}$) is obtained from a two-dimensional (2D) unbinned maximum-likelihood fit [27] to the $M^{\rm tag}_{\rm BC}$ versus $M^{\rm sig}_{\rm BC}$ distribution of the accepted DT candidates. Figure 1 shows the $M^{\rm tag}_{\rm BC}$ versus $M^{\rm sig}_{\rm BC}$ distribution of the accepted DT candidates in data. The signal events concentrate around $M^{\rm tag}_{\rm BC} = M^{\rm sig}_{\rm BC} = M_D$, where M_D is the averaged mass of D [13]. The events with correctly reconstructed D ($\bar{D}$) and incorrectly reconstructed $\bar{D}$ (D), referred to as BKGI, spread along the lines around $M^{\rm sig}_{\rm BC} = M_D$ ($M^{\rm tag}_{\rm BC} = M_D$). Events smeared along the diagonal (BKGII) are mainly from the $e^+e^- \to q\bar{q}$ processes. Events with uncorrelated and incorrectly reconstructed D and $\bar{D}$ (BKGIII) disperse across the whole allowed kinematic region.

In the fit, the probability density functions (PDFs) for signal, BKGI, BKGII, and BKGIII contributions are constructed as $a(x,y)$, $b_x(x) \cdot c_y(y; M^{\rm end}_{\rm BC}, \xi_y) + b_y(y) \cdot c_x(x; M^{\rm end}_{\rm BC}, \xi_x)$, $c_z(z; \sqrt{2}M^{\rm end}_{\rm BC}, \xi_z) \cdot g(k; 0, \sigma_k)$, and $c_x(x; M^{\rm end}_{\rm BC}, \xi_x) \cdot c_y(y; M^{\rm end}_{\rm BC}, \xi_y)$, respectively. Here, $x = M^{\rm sig}_{\rm BC}$, $y = M^{\rm tag}_{\rm BC}$, $z = (x+y)/\sqrt{2}$, and $k = (x-y)/\sqrt{2}$. The PDFs of signal, $a(x,y)$, $b_x(x)$, and $b_y(y)$, are described by the MC-simulated shapes smeared with individual

TABLE I. Requirements of $\Delta E_{\rm sig}$, DT yields in data ($N_{\rm DT}$), detection efficiencies ($\epsilon_{\rm sig}$, including the BFs of η, and π^0 as well as correction factors described later), and the obtained BFs ($\mathcal{B}_{\rm sig}$). The first nine modes are D^0 decays and the others are D^+ decays. For $\mathcal{B}_{\rm sig}$, numbers in the first and second parentheses are the last two digits of the statistical and systematic uncertainties, respectively. For $N_{\rm DT}$, uncertainties are statistical only.

Decay	$\Delta E_{\rm sig}$ (MeV)	$N_{\rm DT}$	$\epsilon_{\rm sig}$ (%)	$\mathcal{B}_{\rm sig}$ ($\times 10^{-4}$)
$\pi^+\pi^-\pi^0$	$(-62, 36)$	12792.6(120.1)	40.91	134.3(13)(16)
$\pi^+\pi^-2\pi^0$	$(-75, 37)$	3801.3(70.6)	16.29	100.2(19)(24)
$\pi^+\pi^-2\eta$	$(-37, 29)$	42.5(6.7)	2.14	8.5(13)(04)
$4\pi^0$	$(-105, 41)$	96.0(11.5)	5.41	7.6(09)(07)
$3\pi^0\eta$	$(-82, 40)$	155.3(14.7)	2.83	23.6(22)(17)
$2\pi^+2\pi^-\pi^0$	$(-52, 33)$	942.4(40.0)	11.70	34.6(15)(15)
$2\pi^+2\pi^-\eta$	$(-36, 28)$	48.5(7.8)	3.46	6.0(10)(06)
$\pi^+\pi^-3\pi^0$	$(-76, 39)$	182.7(20.9)	5.13	15.3(17)(13)
$2\pi^+2\pi^-2\pi^0$	$(-64, 36)$	350.0(22.9)	3.15	47.7(31)(21)
$2\pi^+\pi^-$	$(-30, 28)$	2579.0(57.6)	50.63	32.7(07)(05)
$\pi^+2\pi^0$	$(-96, 44)$	1963.9(51.6)	27.33	46.1(12)(09)
$2\pi^+\pi^-\pi^0$	$(-59, 35)$	4614.4(83.1)	25.42	116.5(21)(21)
$\pi^+3\pi^0$	$(-86, 39)$	573.7(30.2)	8.83	41.7(22)(13)
$3\pi^+2\pi^-$	$(-37, 33)$	462.1(28.7)	16.26	18.2(11)(10)
$2\pi^+\pi^-2\pi^0$	$(-74, 39)$	1207.1(45.4)	7.21	107.4(40)(30)
$2\pi^+\pi^-\pi^0\eta$	$(-51, 33)$	191.4(15.9)	3.17	38.8(32)(12)
$\pi^+4\pi^0$	$(-90, 41)$	56.7(10.4)	1.87	19.5(36)(23)
$\pi^+3\pi^0\eta$	$(-66, 37)$	79.7(10.9)	1.77	28.9(40)(22)
$3\pi^+2\pi^-\pi^0$	$(-49, 34)$	182.8(17.3)	5.02	23.4(22)(15)
$2\pi^+\pi^-3\pi^0$	$(-66, 37)$	185.9(17.0)	3.49	34.2(31)(16)

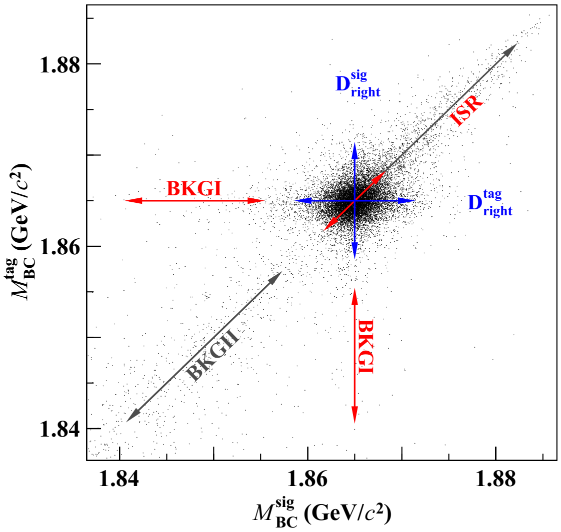

FIG. 1. The $M_{\rm BC}^{\rm tag}$ versus $M_{\rm BC}^{\rm sig}$ distribution of the accepted DT candidates of $D^0 \to \pi^+\pi^-\pi^0$ in data. Here, the ISR denotes initial state radiation, which spreads along the diagonal direction and extends to the higher $M_{\rm BC}$ side. The $D^{\rm sig}_{\rm right}$ and $D^{\rm tag}_{\rm right}$ denote the signal spreading around $M_{\rm BC}^{\rm sig} = M_D$ and $M_{\rm BC}^{\rm tag} = M_D$.

Gaussian resolution function with parameters derived from the corresponding one-dimensional $M_{\rm BC}$ fits, to consider resolution difference between data and MC simulation. The $c_f(f; M_{\rm BC}^{\rm end}, \xi_f)$ is an ARGUS function [26] (f denotes x, y, or z), where the end point $M_{\rm BC}^{\rm end} = 1.8865$ GeV$/c^2$ is fixed in the fit. The Gaussian function $g(k; 0, \sigma_k)$ has a mean of zero and a standard deviation parametrized by $\sigma_k = \sigma_0 \cdot (\sqrt{2}M_{\rm BC}^{\rm end} - z)^p$, where σ_0 and p are fit parameters. In addition, the yields and shapes of the peaking background (PBKG) components, which are mainly from D decays into the same final state as a signal mode but involve $K_S^0 \to \pi^+\pi^-$ or $\pi^0\pi^0$ and $K^- \to \pi^-\pi^0$ decay, are fixed based on MC simulations and the known BFs of various PBKG components [13,28]. Relative to the corresponding signal yields, the PBKG components are 9.5%, 18.2%, and 36.2% for $D^+ \to \pi^+4\pi^0$, $D^0 \to 2\pi^+2\pi^-\pi^0$, and $D^0 \to \pi^+\pi^-3\pi^0$, respectively, and range from 0.1% to 6.3% for the other signal decays.

The $M_{\rm BC}^{\rm tag}$ and $M_{\rm BC}^{\rm sig}$ projections of the 2D fits of the DT candidates reconstructed from data are shown in Fig. 2 and the fitted DT yields are summarized in Table I.

To determine the signal efficiencies ($\epsilon_{\rm sig}$), the three-body decays are simulated with a modified data-driven generator BODY3 [18], which was developed to simulate different intermediate states in data for a given three-body final state. The Dalitz plot from data, corrected for backgrounds and efficiencies, is taken as input for the BODY3 generator. The efficiencies across phase space are obtained with MC samples generated according to a phase space distribution. Each of the four-body and five-body decays is simulated with a mixed signal MC sample. These decays generated with phase space models including contributions from η, ω, η', $\rho(770)$, $a_0(980)$, $a_1(1260)$, $b_1(1235)$, and ϕ intermediate states are mixed with fractions obtained by examining the corresponding invariant mass spectra. The data distributions for momenta and $\cos\theta$ (where θ is the polar angle of particle in the e^+e^- rest frame) of the daughter particles, and the invariant masses of each of the two-body and multibody particle combinations agree with the MC simulations. As an example, Fig. 3 shows the comparisons for the $D^0 \to \pi^+\pi^-\pi^0$ candidates. Some comparisons of the other decay modes can be found in the Supplemental Material [29]. The imperfect data-MC consistencies in the $\pi\pi$ mass spectra will be considered as sources of systematic uncertainties related to the MC generator and K_S^0 rejection in the next section.

The results for $N_{\rm DT}$, $\epsilon_{\rm sig}$, and the extracted BFs are summarized in Table I. For each signal decay, the minimum statistical significance is 6.8 standard deviations for the $D^+ \to \pi^+4\pi^0$ mode. The signal efficiencies have been corrected by the data-MC differences in the selection efficiencies of $\pi^\pm$ tracking, particle identification (PID) procedures and the reconstruction of π^0 or η.

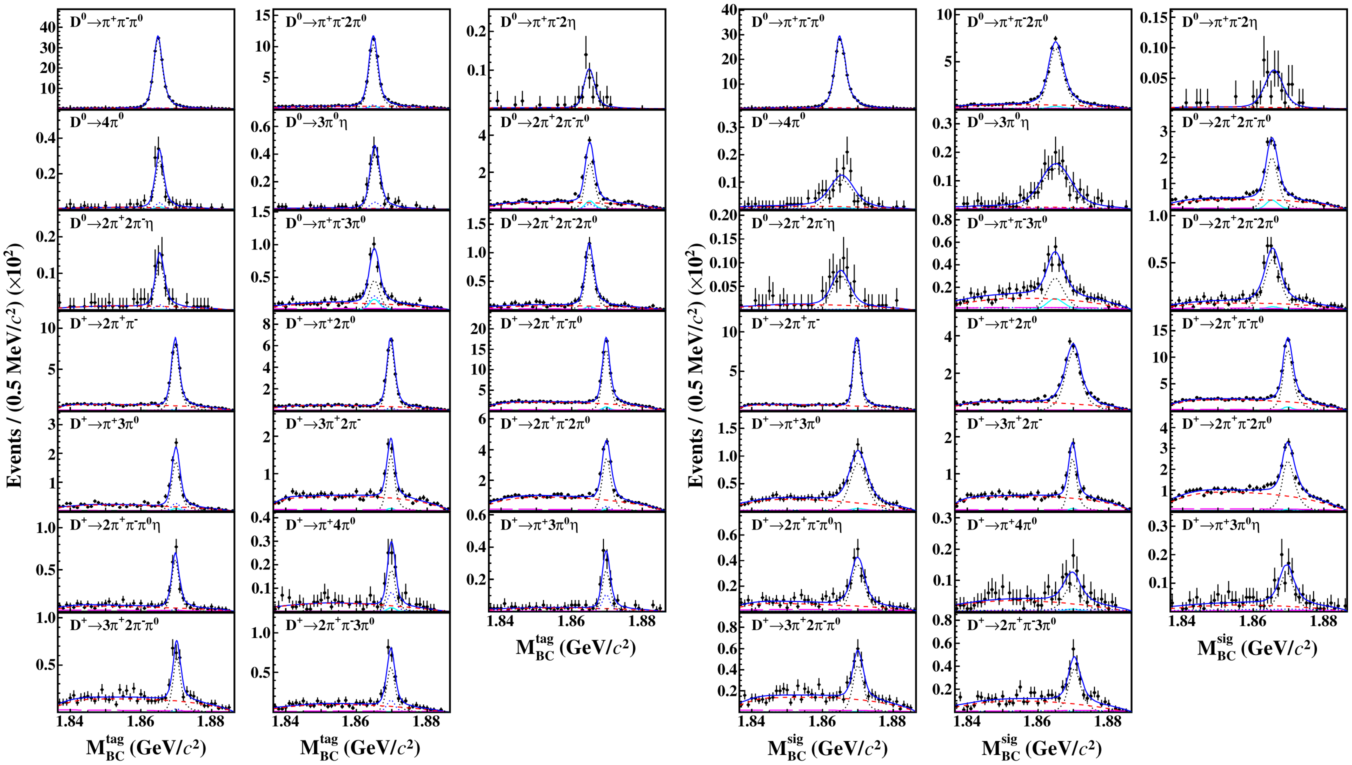

FIG. 2. Projections of $M_{\rm BC}^{\rm tag}$ (left) and $M_{\rm BC}^{\rm sig}$ (right) of the 2D fits to the DT candidate events. Points with error bars are data and blue solid curves are the fit results. Black dotted, cyan blue solid, blue dotted, red dotted, and pink long-dashed correspond to the fitted signal, fixed peaking background, BKGI, BKGII, and BKGIII components, respectively.

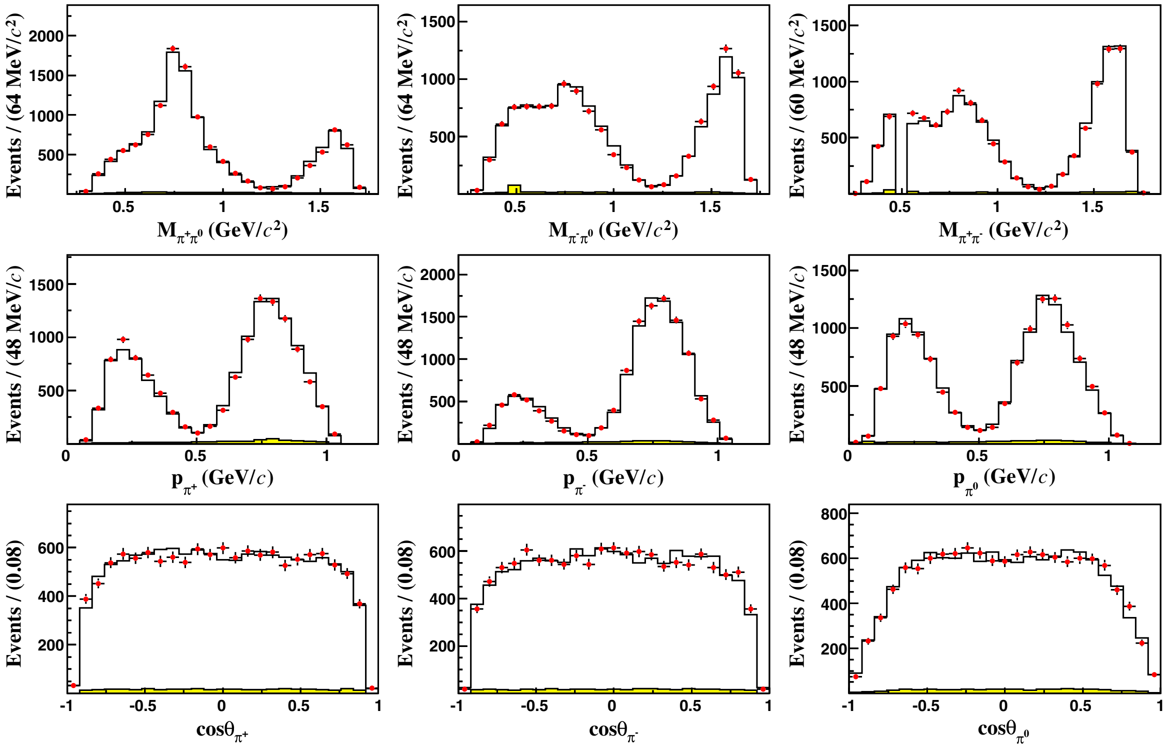

FIG. 3. Comparisons of the distributions of invariant masses of two-body particle combinations, momenta and $\cos\theta$ of daughter particles for the $D^0\to\pi^+\pi^-\pi^0$ candidates between data (points with error bars) and the BODY3 signal MC events (black solid line histograms) plus the MC-simulated backgrounds from the inclusive MC sample (yellow filled histograms).

V. SYSTEMATIC UNCERTAINTIES

The systematic uncertainties relative to the obtained BFs are discussed below. In the BF determinations using Eq. (1), all uncertainties from selecting the ST $\bar{D}$ candidates are canceled in the ratio. Systematic uncertainties in the total yields of ST $\bar{D}$ mesons related to the $M_{\rm BC}^{\rm tag}$ fits to the ST $\bar{D}$ candidates were previously estimated to be 0.5% for both neutral and charged $\bar{D}$ [30–32].

The tracking and PID efficiencies of $\pi^\pm$ are investigated using other DT $D\bar{D}$ hadronic events. The differences of efficiencies between data and MC simulation are weighted by the corresponding $\pi^\pm$ momentum spectra of signal MC events. The systematic uncertainties due to tracking and PID efficiencies are assigned to be (0.2–0.4)% per $\pi^\pm$, based on the residual statistical uncertainties of the measured data-MC differences.

The π^0 reconstruction efficiency, which includes the effects of the photon selection, the π^0 mass window and the kinematic fit on $\pi^0 \to \gamma\gamma$, is studied with the DT $D\bar{D}$ hadronic decay samples of $D^0 \to K^-\pi^+$, $K^-\pi^+\pi^+\pi^-$ versus $\bar{D}^0 \to K^+\pi^-\pi^0$, $K_S^0\pi^0$ following Refs. [30,31]. After correcting our signal efficiencies by the momentum weighted data-MC differences, the residual uncertainties are assigned as the systematic uncertainties, which are (0.4–0.9)% per π^0 for various signal decays. Because of limited η statistics, the systematic uncertainty for η reconstruction is assigned by referring to that of π^0.

The systematic uncertainty in the 2D fit to the $M_{\rm BC}^{\rm tag}$ versus $M_{\rm BC}^{\rm sig}$ distribution is examined by varying the smeared Gaussian function ($\pm 1\sigma$), the end point of the ARGUS function (± 0.2 MeV/c^2), and the fixed PBKG yields ($\pm 1\sigma$ of the quoted BF). Adding the changes from these three sources in quadrature yields the corresponding systematic uncertainties.

The systematic uncertainty due to the $\Delta E_{\rm sig}$ requirement ranges from (0.1–1.3)% depending on the signal mode. They are evaluated from the efficiency differences obtained with and without smearing the $\Delta E_{\rm sig}$ distributions for signal MC events with parameters derived from $D^0 \to \pi^+\pi^-\pi^0$, $D^0 \to \pi^+\pi^-2\pi^0$, $D^+ \to \pi^+2\pi^0$, and $D^+ \to 2\pi^+\pi^-\pi^0$ to get the data-MC differences.

The systematic uncertainty due to the BODY3 generator is considered by varying the number of bins by ±20% and the systematic uncertainty in the mixed MC model is assigned by varying the fractions of various components by $\pm 1\sigma$ of the quoted BF, when available. Unmeasured components are varied by ±25%, beyond which comparisons with observed mass spectra are unsatisfactory. The largest change of the signal efficiencies, (0.2–5.7)% for various signal modes, are assigned as the corresponding systematic uncertainties.

The systematic uncertainties due to the mass window applied to reject K_S^0 events are cross-checked by examining the changes of the BFs by varying the corresponding boundaries of the window by ± 5 MeV/c^2, which is about $\pm 1\sigma$ of the fitted resolution. If the difference of the BF is greater than the statistical uncertainty on the difference (taking the correlated samples into account), it is assigned as the corresponding systematic uncertainty. Otherwise, it is neglected.

The measurements of the BFs of the neutral D decays are affected by the quantum correlation (QC) effect [33]. To take this effect into account, the CP-even fractions in various decays are needed. The $D^0 \to 4\pi^0$ and $D^0 \to 3\pi^0\eta$ final states are both CP-even eigenstates. For $D^0 \to \pi^+\pi^-\pi^0$, its CP-even fraction has been determined to be 0.973 ± 0.017 [34]. For $D^0 \to \pi^+\pi^-2\pi^0$, $D^0 \to 2\pi^+2\pi^-\pi^0$, $D^0 \to \pi^+\pi^-3\pi^0$, and $D^0 \to 2\pi^+2\pi^-2\pi^0$, the CP-even fractions are estimated by the CP-even tag $D^0 \to K^+K^-$ and the CP-odd tag $D^0 \to K_S^0\pi^0$.

The obtained ST yields of the CP-even tag of $\bar{D}^0 \to K^+K^-$ and the CP-odd tag of $\bar{D}^0 \to K_S^0\pi^0$ are $S^-_{\rm measured} = 57779 \pm 287$ and $S^+_{\rm measured} = 70512 \pm 311$, respectively, which are derived from the fits to individual $M_{\rm BC}^{\rm tag}$ distributions of the accepted ST candidates. The DT yields tagged by $CP\pm$ tags from the 2D fits to the $M_{\rm BC}^{\rm tag}$ versus $M_{\rm BC}^{\rm sig}$ distributions of the accepted DT candidates, and the QC factors obtained with the same method as described in

TABLE II. The DT yields tagged by $CP \mp$ tags ($M^{\pm}_{\rm measured}$), the $CP+$ fractions (f_{CP+}), and the QC factors ($f_{\rm QC}$). The f_{CP+} for $D^0 \to \pi^+\pi^-\pi^0$ is quoted from Ref. [34]; the f_{CP+} values for $D^0 \to \pi^+\pi^-2\pi^0$, $D^0 \to 2\pi^+2\pi^-\pi^0$, $D^0 \to \pi^+\pi^-3\pi^0$, and $D^0 \to 2\pi^+2\pi^-2\pi^0$ are determined in this work; and the f_{CP+} values for $D^0 \to 4\pi^0$ and $D^0 \to 3\pi^0\eta$ are taken to be 1 based on theoretical expectations. The uncertainties are statistical only.

Decay	$M^-_{\rm measured}$	$M^+_{\rm measured}$	f_{CP+}	$f_{\rm QC}$ (%)
$D^0 \to \pi^+\pi^-\pi^0$	⋯	⋯	0.973 ± 0.017 [34]	93.5 ± 0.5
$D^0 \to \pi^+\pi^-2\pi^0$	65.7 ± 11.1	169.8 ± 13.9	0.682 ± 0.077	97.4 ± 0.7
$D^0 \to 4\pi^0$	⋯	⋯	1	93.1 ± 0.5
$D^0 \to 3\pi^0\eta$	⋯	⋯	1	93.1 ± 0.5
$D^0 \to 2\pi^+2\pi^-\pi^0$	37.8 ± 8.3	35.5 ± 6.6	0.438 ± 0.104	100.9 ± 0.9
$D^0 \to \pi^+\pi^-3\pi^0$	$5.2^{+3.5}_{-2.8}$	$6.8^{+3.4}_{-2.7}$	$0.520^{+0.338}_{-0.269}$	$99.7^{+3.0}_{-2.4}$
$D^0 \to 2\pi^+2\pi^-2\pi^0$	$3.5^{+2.8}_{-2.1}$	15.9 ± 3.7	$0.790^{+0.269}_{-0.255}$	$95.9^{+2.2}_{-2.1}$

TABLE III. Systematic uncertainties (%) in the measurements of the BFs for various decay modes.

	$D^0 \to$									$D^+ \to$
Source	$\pi^+\pi^-\pi^0$	$\pi^+\pi^-2\pi^0$	$\pi^+\pi^-2\eta$	$4\pi^0$	$3\pi^0\eta$	$2\pi^+2\pi^-\pi^0$	$2\pi^+2\pi^-\eta$	$\pi^+\pi^-3\pi^0$	$2\pi^+2\pi^-2\pi^0$	$2\pi^+\pi^-$
$N_{\rm tag}$	0.5	0.5	0.5	0.5	0.5	0.5	0.5	0.5	0.5	0.5
$\pi^\pm$ tracking	0.4	0.4	0.7	…	…	0.8	1.0	0.4	0.8	0.6
$\pi^\pm$ PID	0.4	0.4	0.4	…	…	0.8	0.8	0.4	0.8	0.6
π^0/η reconstruction	0.4	1.3	1.6	2.3	2.5	0.6	0.7	1.9	1.3	…
2D fit	0.3	0.6	4.4	3.4	4.7	1.7	4.0	3.5	2.3	0.3
$\Delta E^{\rm sig}$ cut	0.1	0.1	1.3	0.1	0.1	0.2	0.8	0.1	0.1	0.3
MC generator	0.6	1.5	0.2	3.4	2.8	1.1	1.5	5.3	1.4	0.8
K^0_S rejection	0.1	0.4	…	7.4	3.5	3.2	8.1	4.7	1.6	0.5
Strong phase	0.5	0.7	…	0.5	0.5	0.9	…	3.0	2.2	…
MC statistics	0.2	0.4	0.5	0.8	0.7	0.5	0.6	0.8	1.0	0.2
Daughter $\mathcal{B}$	0.03	0.07	1.02	0.14	0.52	0.03	0.51	0.10	0.07	…
Total	1.2	2.4	5.1	9.2	7.0	4.2	9.4	8.7	4.3	1.4

	$D^+ \to$									
Source	$\pi^+2\pi^0$	$2\pi^+\pi^-\pi^0$	$\pi^+3\pi^0$	$3\pi^+2\pi^-$	$2\pi^+\pi^-2\pi^0$	$2\pi^+\pi^-\pi^0\eta$	$\pi^+4\pi^0$	$\pi^+3\pi^0\eta$	$3\pi^+2\pi^-\pi^0$	$2\pi^+\pi^-3\pi^0$
$N_{\rm tag}$	0.5	0.5	0.5	0.5	0.5	0.5	0.5	0.5	0.5	0.5
$\pi^\pm$ tracking	0.2	0.6	0.2	1.1	0.6	0.8	0.2	0.2	1.2	0.6
$\pi^\pm$ PID	0.2	0.6	0.2	1.0	0.6	0.6	0.2	0.2	1.0	0.6
π^0/η reconstruction	1.0	0.6	1.8	…	1.4	1.4	2.7	3.4	0.8	2.5
2D fit	0.3	0.6	1.7	2.1	1.8	2.3	3.1	3.4	2.8	2.7
$\Delta E^{\rm sig}$ cut	0.1	0.1	0.1	0.2	0.1	0.5	0.1	0.1	0.4	0.1
MC generator	1.5	0.8	1.5	3.0	0.7	0.3	4.2	5.7	0.5	1.7
K^0_S rejection	…	0.8	1.1	3.4	0.8	…	10.2	…	5.6	2.2
Strong phase	…	…	…	…	…	…	…	…	…	…
MC statistics	0.3	0.3	0.6	0.4	0.6	0.6	1.3	0.8	0.8	0.9
Daughter $\mathcal{B}$	0.07	0.03	0.10	…	0.07	0.51	0.14	0.52	0.03	0.10
Total	1.9	1.8	3.2	5.3	2.8	3.1	11.9	7.5	6.6	4.8

Ref. [35] and the necessary parameters quoted from Refs. [36–38] are summarized in Table II. After correcting the signal efficiencies by the individual factors, the residual uncertainties are assigned as systematic uncertainties.

The uncertainties of MC statistics for various signal decays, (0.2–1.3)%, are considered as a systematic uncertainty. The uncertainties of the daughter BFs of $\eta \to \gamma\gamma$ and $\pi^0 \to \gamma\gamma$ are 0.51% and 0.03%, respectively [13].

Adding all individual effects for each signal decay quadratically yields the total systematic uncertainties to be (1.2–11.9)% depending on the signal mode. Table III summarizes the systematic uncertainties for various sources.

VI. ASYMMETRIES OF CHARGE-SEPARATED BFS

For the six decay modes with the highest yields, the BFs of D and $\bar{D}$ decays, $\mathcal{B}^{+}_{\rm sig}$ and $\mathcal{B}^{-}_{\overline{\rm sig}}$, are measured separately. Their asymmetry is determined by $\mathcal{A}^{\rm sig}_{CP} = \frac{\mathcal{B}^{+}_{\rm sig} - \mathcal{B}^{-}_{\overline{\rm sig}}}{\mathcal{B}^{+}_{\rm sig} + \mathcal{B}^{-}_{\overline{\rm sig}}}$. The obtained BFs and asymmetries are summarized in Table IV. We find no statistically significant CP violation. Several systematic uncertainties cancel in the asymmetry: the tracking and PID efficiencies of $\pi^+\pi^-$ pairs, the π^0 and η reconstruction, the daughter BFs, the K^0_S rejection windows, the MC modeling, and the strong phase of D^0 decays. The other systematic uncertainties, e.g., the tracking and PID efficiencies of bachelor $\pi^\pm$ for $D^\pm$ decays, are estimated separately as above.

TABLE IV. Charge-separated BFs ($\mathcal{B}^{+}_{\rm sig}$ and $\mathcal{B}^{-}_{\overline{\rm sig}}$), and their asymmetries ($\mathcal{A}^{\rm sig}_{CP}$). The first and second uncertainties are statistical and systematic, respectively, for $\mathcal{A}^{\rm sig}_{CP}$; while uncertainties for $\mathcal{B}^{+}_{\rm sig}$ and $\mathcal{B}^{-}_{\overline{\rm sig}}$ are only statistical.

Decay	$\mathcal{B}^{+}_{\rm sig}(\times 10^{-4})$	$\mathcal{B}^{-}_{\overline{\rm sig}}(\times 10^{-4})$	$\mathcal{A}^{\rm sig}_{CP}$ (%)
$\pi^+\pi^-\pi^0$	134.8 ± 1.8	133.3 ± 1.8	$+0.6 \pm 0.9 \pm 0.4$
$\pi^+\pi^-2\pi^0$	97.6 ± 2.6	102.7 ± 2.7	$-2.5 \pm 1.9 \pm 0.7$
$2\pi^+\pi^-$	33.1 ± 1.0	32.3 ± 1.0	$+1.2 \pm 2.2 \pm 0.6$
$\pi^+2\pi^0$	48.3 ± 1.8	43.2 ± 1.7	$+5.6 \pm 2.7 \pm 0.5$
$2\pi^+\pi^-\pi^0$	116.7 ± 3.0	116.0 ± 3.0	$+0.3 \pm 1.8 \pm 0.8$
$2\pi^+\pi^-2\pi^0$	102.7 ± 5.6	111.6 ± 5.8	$-4.2 \pm 3.8 \pm 1.3$

VII. SUMMARY

To summarize, by analyzing 2.93 fb^{-1} of e^+e^- annihilation data recorded at $\sqrt{s} = 3.773$ GeV with the BESIII detector, we present the first absolute measurements of the BFs of twenty Cabibbo-suppressed hadronic $D^{0(+)}$ decays involving multiple pions. For $D^0 \to \pi^+\pi^-\pi^0$, $\pi^+\pi^-2\pi^0$, $2\pi^+2\pi^-\pi^0$, and $D^+ \to 2\pi^+\pi^-$, $\pi^+2\pi^0$, $2\pi^+\pi^-\pi^0$, $3\pi^+2\pi^-$, the BF precisions are improved by factors of 1.2–2.9 compared to the world average values based on relative measurements. For the other 13 decay modes, the BFs are measured for the first time. The reported BFs offer important input for reliable estimations of potential background sources in the precision measurements of B and D decays, especially to properly evaluate the tensions found in the LFU tests with semileptonic B decays. Amplitude analyses of these multibody decays with larger data samples available in the near future [39,40] will open an opportunity to precisely extract more quasi-two-body hadronic $D^{0(+)}$ decay rates, e.g., $D^+ \to \rho^+\pi^0$. Detailed knowledge of these hadronic $D^{0(+)}$ decays is essential to deeply explore quark U-spin and SU(3)-flavor symmetry breaking effects and thereby improve the predictions of CP violation in the charm sector [2,41,42]. Additionally, the asymmetries of the charge-conjugated BFs of the six $D^{0(+)}$ decays with highest signal yields are determined. No statistically significant CP violation is observed.

ACKNOWLEDGMENTS

The BESIII collaboration thanks the staff of BEPCII and the IHEP computing center for their strong support. This work is supported in part by National Key R&D Program of China under Contracts No. 2020YFA0406400 and No. 2020YFA0406300; National Natural Science Foundation of China (NSFC) under Contracts No. 11625523, No. 11635010, No. 11735014, No. 11822506, No. 11835012, No. 11935015, No. 11935016, No. 11935018, No. 11961141012, No. 12022510, No. 12025502, No. 12035009, No. 12035013, No. 12061131003, No. 12192260, No. 12192261, No. 12192262, No. 12192263, No. 12192264, No. 12192265; the Chinese Academy of Sciences (CAS) Large-Scale Scientific Facility Program; Joint Large-Scale Scientific Facility Funds of the NSFC and CAS under Contracts No. U1732263, No. U1832207, No. U1932102; CAS Key Research Program of Frontier Sciences under Contract No. QYZDJ-SSW-SLH040; 100 Talents Program of CAS; INPAC and Shanghai Key Laboratory for Particle Physics and Cosmology; ERC under Contract No. 758462; European Union Horizon 2020 research and innovation program under Marie Sklodowska-Curie Grant Agreement No. 894790; German Research Foundation DFG under Contract No. 443159800, Collaborative Research Center CRC 1044, FOR 2359, FOR 2359, GRK 2149; Istituto Nazionale di Fisica Nucleare, Italy; Ministry of Development of Turkey under Contract No. DPT2006K-120470; National Science and Technology fund; Olle Engkvist Foundation under Contract No. 200-0605; STFC (United Kingdom); The Knut and Alice Wallenberg Foundation (Sweden) under Contract No. 2016.0157; The Royal Society, U.K. under Contracts No. DH140054, No. DH160214; The Swedish Research Council; U.S. Department of Energy under Contracts No. DE-FG02-05ER41374, No. DE-SC-0012069.

---

[1] R. Aaij *et al.* (LHCb Collaboration), Synergy of BESIII and LHCb physics programs, Report No. LHCb-PUB-2016-025.

[2] H. N. Li, C. D. Lü, and F. S. Yu, Phys. Rev. D **86**, 036012 (2012).

[3] H. Y. Cheng and C. W. Chiang, Phys. Rev. D **100**, 093002 (2019).

[4] I. I. Bigi, A. Paul, and S. Recksiegel, J. High Energy Phys. 06 (2011) 089.

[5] G. Isidori, J. F. Kamenik, Z. Ligeti, and G. Perez, Phys. Lett. B **711**, 46 (2012).

[6] J. Brod, A. L. Kagan, and J. Zupan, Phys. Rev. D **86**, 014023 (2012).

[7] H. Y. Cheng and C. W. Chiang, Phys. Rev. D **86**, 014014 (2012).

[8] H. N. Li, C. D. Lü, and F. S. Yu, arXiv:1903.10638.

[9] M. Saur and F. S. Yu, Sci. Bull. **65**, 1428 (2020).

[10] R. Aaij *et al.* (LHCb Collaboration), Phys. Rev. Lett. **122**, 211803 (2019).

[11] B. Aubert *et al.* (*BABAR* Collaboration), Phys. Rev. D **72**, 071102 (2005).

[12] M. Ablikim *et al.* (BESIII Collaboration), Chin. Phys. C **37**, 123001 (2013).

[13] P. A. Zyla *et al.* (Particle Data Group), Prog. Theor. Exp. Phys. **2020**, 083C01 (2020).

[14] M. Ablikim *et al.* (BESIII Collaboration), Nucl. Instrum. Methods Phys. Res., Sect. A **614**, 345 (2010).

[15] C. H. Yu *et al.*, in *Proceedings of IPAC2016, Busan, Korea* (JACoW, Geneva, Switzerland, 2016).

[16] S. Agostinelli *et al.* (GEANT4 Collaboration), Nucl. Instrum. Methods Phys. Res., Sect. A **506**, 250 (2003).

[17] S. Jadach, B. F. L. Ward, and Z. Was, Comput. Phys. Commun. **130**, 260 (2000); Phys. Rev. D **63**, 113009 (2001).

[18] D. J. Lange, Nucl. Instrum. Methods Phys. Res., Sect. A **462**, 152 (2001); R. G. Ping, Chin. Phys. C **32**, 599 (2008).

[19] J. C. Chen, G. S. Huang, X. R. Qi, D. H. Zhang, and Y. S. Zhu, Phys. Rev. D **62**, 034003 (2000).

[20] R.-L. Yang, R. G Ping, and H. Chen, Chin. Phys. Lett. **31**, 061301 (2014).

[21] E. Richter-Was, Phys. Lett. B **303**, 163 (1993).

[22] H. B. Li and X. R. Lyu, Natl. Sci. Rev. **8**, nwab181 (2021).

[23] M. Ablikim *et al.* (BESIII Collaboration), Phys. Rev. D **101**, 052009 (2020).

[24] M. Ablikim *et al.* (BESIII Collaboration), Phys. Rev. Lett. **124**, 241803 (2020).

[25] M. Ablikim *et al.* (BESIII Collaboration), Phys. Lett. B **734**, 227 (2014).

[26] H. Albrecht *et al.* (ARGUS Collaboration), Phys. Lett. B **241**, 278 (1990).

[27] S. Dobbs *et al.* (CLEO Collaboration), Phys. Rev. D **76**, 112001 (2007).

[28] M. Ablikim *et al.* (BESIII Collaboration), Phys. Rev. D **106**, 032002 (2022).

[29] See Supplemental Material at http://link.aps.org/supplemental/10.1103/PhysRevD.106.092005 for the comparisons of some typical distributions of the DT candidates between data and MC simulation.

[30] M. Ablikim *et al.* (BESIII Collaboration), Eur. Phys. J. C **76**, 369 (2016).

[31] M. Ablikim *et al.* (BESIII Collaboration), Chin. Phys. C **40**, 113001 (2016).

[32] M. Ablikim *et al.* (BESIII Collaboration), Phys. Rev. Lett. **121**, 171803 (2018).

[33] G. Wilkinson, Sci. Bull. **66**, 2251 (2021).

[34] S. Malde, C. Thomas, G. Wilkinson, P. Naik, C. Prouve, J. Rademacker, J. Libby, M. Nayak, T. Gershon, and R. A. Briere, Phys. Lett. B **747**, 9 (2015).

[35] M. Ablikim *et al.* (BESIII Collaboration), Phys. Rev. D **100**, 072006 (2019).

[36] T. Gershon, J. Libby, and G. Wilkinson, Phys. Lett. B **750**, 338 (2015).

[37] T. Evans, S. T. Harnew, J. Libby, S. Malde, J. Rademacker, and G. Wilkinson, Phys. Lett. B **757**, 520 (2016); **765**, 402(E) (2017).

[38] Heavy Flavor Averaging Group (HFLAV Collaboration), http://www.slac.stanford.edu/xorg/hflav/charm/.

[39] M. Ablikim *et al.* (BESIII Collaboration), Chin. Phys. C **44**, 040001 (2020).

[40] E. Kou *et al.* (Belle II Collaboration), Prog. Theor. Exp. Phys. **2019**, 123C01 (2019); **2020**, 029201(E) (2020).

[41] H. Y. Cheng and C. W. Chiang, Phys. Rev. D **81**, 074021 (2010).

[42] Q. Qin, H. N. Li, C. D. Lü, and F. S. Yu, Phys. Rev. D **89**, 054006 (2014).